

Change of the favored routes of EI MS fragmentation when proceeding from N^1 , N^1 -dimethyl- N^2 -arylformamidines to 1,1,3,3-tetraalkyl-2-arylguanidines: substituent effects

Ewa D. Raczyńska,^{a*} Mariusz Makowski,^b Jean-François Gal^{c*} and Pierre-Charles Maria^c

Although series of N^1 , N^1 -dimethyl- N^2 -arylformamidines and of 1,1,3,3-tetraalkyl-2-arylguanidines are structurally analogous and similar electron-ionization mass spectral fragmentation may be expected, they display important differences in the favored routes of fragmentation and consequently in substituent effects on ion abundances. In the case of formamidines, the cyclization-elimination process (initiated by nucleophilic attack of the N -amino atom on the 2-position of the phenyl ring) and formation of the cyclic benzimidazolium $[M-H]^+$ ions dominates, whereas the loss of the NR_2 group is more favored for guanidines. In order to gain information on the most probable structures of the principal fragments, quantum-chemical calculations were performed on a selected set. A good linear relation between $\log\{[M-H]^+ / [M]^{+\bullet}\}$ and σ_p^+ constants of substituent at *para* position in the phenyl ring occurs solely for formamidines ($r = 0.989$). In the case of guanidines, this relation is not significant ($r = 0.659$). A good linear relation is found between $\log\{[M-NMe_2]^+ / [M]^{+\bullet}\}$ and σ_p^+ constants ($r = 0.993$). Copyright © 2010 John Wiley & Sons, Ltd.

Keywords: electron-ionization mass spectra; fragmentation; N^1 , N^1 -dimethyl- N^2 -arylformamidines; 1,1,3,3-tetraalkyl-2-arylguanidines; substituent effects; quantum-chemical calculations

Introduction

Amidines and guanidines are well known for their strong basicity in the gas phase as well as in solution.^[1–5] Their exceptional basicity is a consequence of very effective $n-\pi$ conjugation between the amino- and imino-nitrogen atoms in the amidine and guanidine groups (Scheme 1). For monofunctional derivatives, the N -imino atom is always the favored site of protonation. The protonation leads to very stable amidinium and guanidinium cations. The gas-phase basicity of amidines and guanidines has been investigated by our group using Fourier transform ion cyclotron resonance mass spectrometry (FT-ICR-MS) and the influence of substituent discussed.^[2,3] We found that relations between gas-phase basicities and substituent constants for guanidines are similar to those for amidines. Cross $n-\pi$ conjugation in guanidines affects solely the slope of the regression line between gas-phase basicities of guanidines and amidines. However, the influence of substituents on the mass spectral fragmentation and ion abundances of amidines and guanidines has not yet been well documented.

For other compounds, there have been a number of attempts to correlate ion abundances in mass spectra with substituent constants^[6,7] in the context of linear free energy (Gibbs energy) relationships (LFER). In the early review,^[6] it was stated that correlations were observed almost exclusively for the intensities of ions which do not retain the substituent. The principal reason

for this is that the ion containing the substituent dissociates further, in ways which depend on the paths induced by the specific structure of each substituent. In the case of amidines, the mass spectrometric fragmentation of N^1 , N^1 -dimethyl- N^2 -arylformamidines (DMAF) has been studied by Bose *et al.*^[8], Grützmaier and Kusche,^[9–12] Marsel and coworkers^[13] and also by our group.^[14] To prove the mechanism proposed for the formation of the benzimidazolium ions during mass spectral fragmentation, Grützmaier and Kusche^[9–12] showed

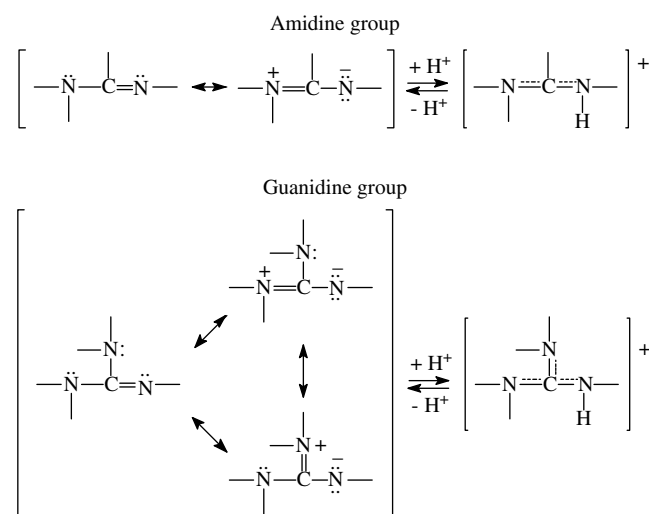
* Correspondence to: Ewa D. Raczyńska, Department of Chemistry, Warsaw University of Life Sciences (SGGW), ul. Nowoursynowska 159c, 02-776 Warszawa, Poland. E-mail: ewa_raczynska@sggw.pl

Jean-François Gal, Laboratoire de Radiochimie, Sciences Analytiques et Environnement, Institute of Chemistry of Nice (FR CNRS 3037), University of Nice - Sophia Antipolis, Parc Valrose, 06108 Nice Cedex 2, France. E-mail: jean.francois.gal@unice.fr

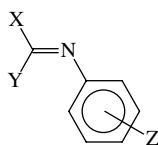
a Department of Chemistry, Warsaw University of Life Sciences (SGGW), ul. Nowoursynowska 159c, 02-776 Warszawa, Poland

b Faculty of Chemistry, University of Gdańsk, ul. Sobieskiego 18, 80-952 Gdańsk, Poland

c Laboratoire de Radiochimie, Sciences Analytiques et Environnement, Institute of Chemistry of Nice (FR CNRS 3037), University of Nice - Sophia Antipolis, Parc Valrose, 06108 Nice Cedex 2, France



Scheme 1. Resonance effects in the amidine and guanidine group.



Compound	No	X	Y	Z
DMAF	1	NMe ₂	H	H
	2	NMe ₂	H	4-NMe ₂
	3	NMe ₂	H	4-OMe
	4	NMe ₂	H	4-Me
	5	NMe ₂	H	4-F
	6	NMe ₂	H	4-Cl
	7	NMe ₂	H	4-CF ₃
	8	NMe ₂	H	4-CN
	9	NMe ₂	H	4-NO ₂
TMAG	10	NMe ₂	NMe ₂	H
	11	NMe ₂	NMe ₂	4-OMe
	12	NMe ₂	NMe ₂	4-Me
	13	NMe ₂	NMe ₂	4-F
	14	NMe ₂	NMe ₂	4-Cl
TEPG	15	NEt ₂	NEt ₂	H

Scheme 2. Guanidines and formamidines studied in this paper.

that the ionization energy (IE) values of the parent molecules are linearly correlated with the Hammett σ constants describing the substituent polar effect, whereas the appearance energy (AE) values do not exhibit any simple relationship. On the other hand, Marsel and coworkers,^[13] investigating also the IE and AE values for formamidines, proposed a linear correlation between the (AE-IE) differences and the Brown's σ^+ constants. Negative slopes found for both 4- and 3-substituted derivatives supported the cyclization-elimination process and the formation of the benzimidazolium ions.

In this paper, we extended the series of DMAF to nine derivatives (**1–9**) – only *p*-substituted at the phenyl ring (Scheme 2) – and we also studied a series of analogous pentasubstituted guanidines, 1,1,3,3-tetramethyl-2-arylguanidines (TMAG **10–14**) and

1,1,3,3-tetraethyl-2-phenylguanidine (TEPG**15**). For all derivatives, standard 70 eV mass spectra have been recorded using FT-ICR-MS. The general routes of mass spectrometric fragmentation were compared. Effects of the substituent Z at the phenyl ring and of the additional dialkylamino group Y at the functional carbon atom in guanidines were analyzed. In an attempt to understand the factors favoring the dissociation routes, the structures of selected fragments were studied by quantum-chemical methods.

Experimental and Computational Details

Chemicals

All compounds studied here were synthesized according to known procedures. DMAFs (**1–9**) were synthesized by heating equimolar amounts of dimethylformamide dimethylacetal with the corresponding substituted aniline for *ca* 30 min at 60 °C as described previously.^[15–17] TMAGs (**10–14**) were obtained using the method of Brederick and Brederick^[18–20] by reaction of 1,1,3,3-tetramethylurea and substituted or unsubstituted aniline in the presence of POCl₃. Similarly, TEPG (**15**) was synthesized using the same method by reaction of 1,1,3,3-tetraethylurea and aniline in the presence of POCl₃. Liquid amidines and guanidines were purified by vacuum distillation and next by preparative gas chromatography (Carlo Erba Fractovap 2400V) at 150–250 °C using 2 m preparative columns (20% SE30). Solid derivatives were purified by sublimation under reduced pressure.

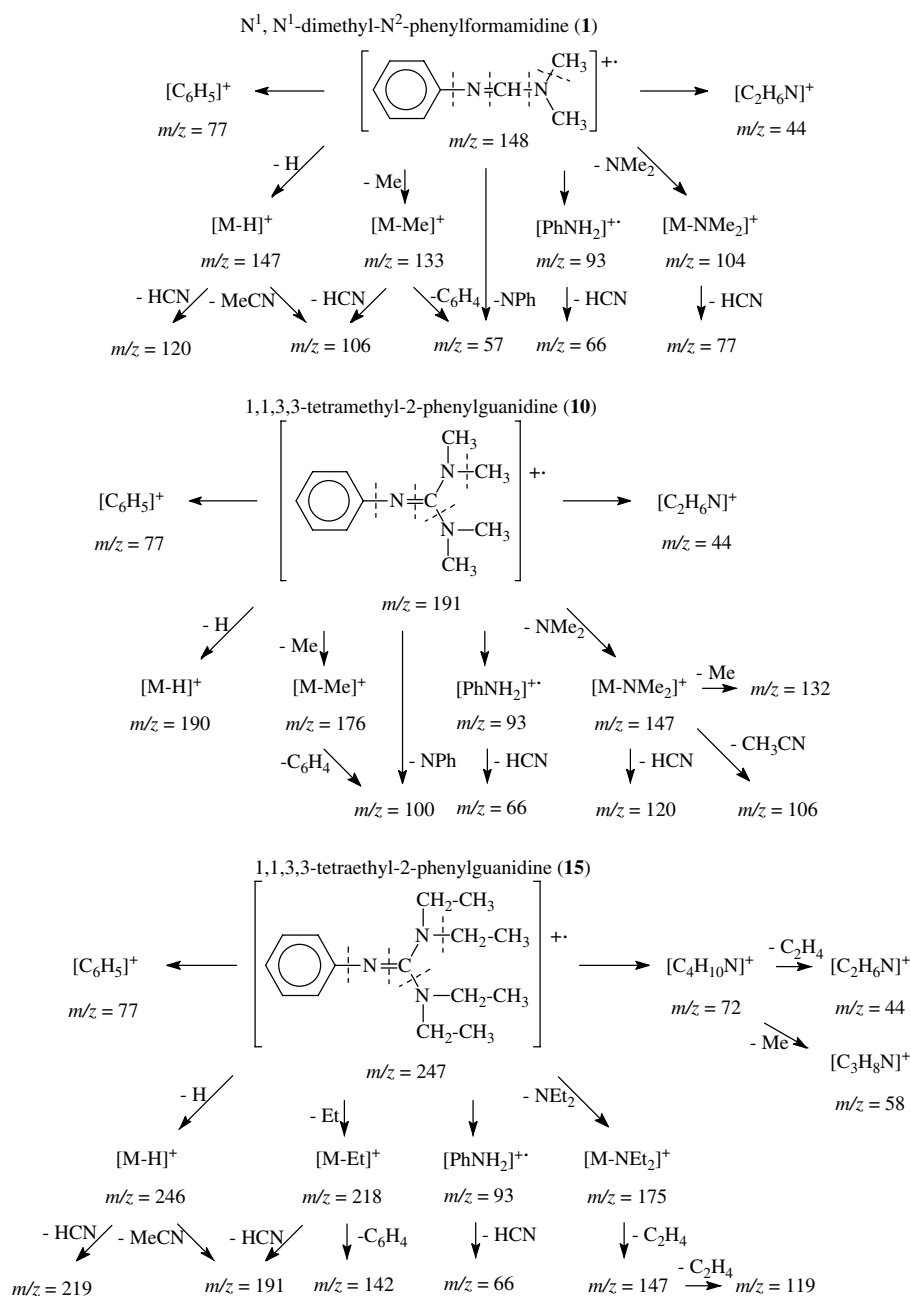
Mass spectrometry

Mass spectra (electron ionization, 70 eV) were recorded using the FT-ICR-MS electromagnet instrument constructed at the University of Nice Sophia Antipolis.^[21] The conditions of measurements were the same as described previously.^[22] The usual mass range was *m/z* 17–400. The spectral resolution was about 1000 at *m/z* 100 with a digital resolution of about 23 Hz (10⁻² at *m/z* 100).

Quantum-chemical calculations

Quantum-chemical calculations were carried out at the Austin model 1 (AM1)^[23] level for fragments indicated in Scheme 3 as [M]⁺, [M-H]⁺ and [M-NMe₂]⁺ of DMAF (**1–9**) and TMAG (**10–15**), and also for the [C₇H₁₆N₃]⁺ fragment of guanidine **15**. Structures of various possible isomers were considered. For AM1 calculations, the HyperChem program was used.^[24] Next, the density functional theory (DFT) method^[25] with the B3LYP (Becke three-parameter hybrid exchange functional and the non-local correlation functional of Lee, Yang and Parr) functional,^[26,27] and the 6-31+G** basis set^[28] were applied to the structures selected at the AM1 level. Geometries of isolated fragments were fully optimized without symmetry constraints. At the energy minima (with real frequencies) of a given species, which corresponded to the conformational preference, the Gibbs (free) energies ($G = H - TS$) were calculated at 298.15 K using the same level of theory. The *G* values include changes in the zero-point energy (ZPE) and thermal corrections (vibrational, rotational and translational) to the enthalpy (*H*) and entropy (*S*). The CN bond lengths and the Mulliken charges for the C and N atoms were also estimated at the DFT level.

Two dissociation curves of the NMe₂ group from N¹,N¹-dimethyl-N²-phenyl-formamidine (**1**) and 1,1,3,3-tetramethyl-2-phenylguanidine (**10**) radical cations [M]⁺ were calculated by carrying out a series of constrained energy minimization with the



Scheme 3. General routes of fragmentation for formamidine **1**, and guanidines **10** and **15**.

C-N distance fixed at a given value and optimizing the remaining degrees of freedom. The fixed distances were from 1.0 to 3.0 Å by steps of 0.1 Å. The steps were 0.05 Å when approaching the minimum energy on the fragmentation plot. Both curves were calculated using the DFT(B3LYP) method and the 6-31+G** basis set. All calculations were performed using the Gaussian 98 program.^[29]

Results and Discussion

EI MS fragmentation for parent compounds (Z = H)

In order to distinguish the effect of $n-\pi$ cross conjugation in guanidines, we compared the general routes of mass spectrometric frag-

mentation (Scheme 3) of *N*¹,*N*¹-dimethyl-*N*²-phenylformamidinium (**1**) with those observed for 1,1,3,3-tetramethyl-2-phenylguanidinium (**10**) and TEPG (**15**). Guanidines **10** and **15** differ only by the nature of the alkyl groups at the amino nitrogen atoms (methyl in **10** and ethyl in **15**). This difference strongly influences gas-phase basicity.^[3] Larger alkyl groups induce stronger basicity. It may also affect bond strength and consequently mass spectrometric fragmentation. Formamidine **1** contains a hydrogen atom at the functional carbon atom, which is replaced by a dialkylamino group for guanidines **10** and **15**. The general routes of mass spectrometric fragmentation of **1** have been proposed by Grützmaier and Kuschel.^[9] Our mass spectrum of **1** is in good agreement with their scheme. Comparison of the mass spectra of guanidines **10** and **15** shows some similarities but also some differences in comparison

Table 1. Selected MS data [m/z (% intensity)] for phenyl derivatives **1**, **10** and **15**

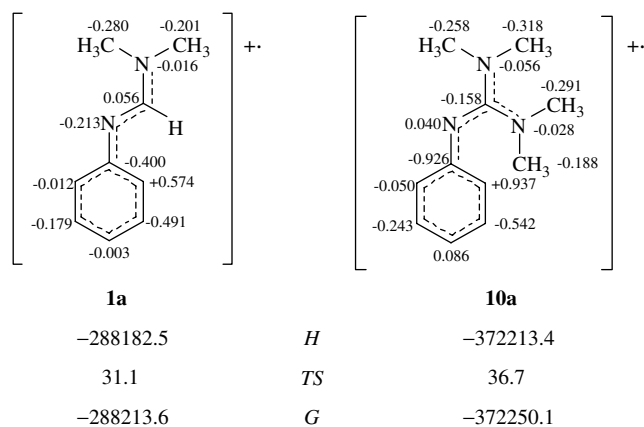
Ion	1	10	15
$[M]^+$	148 (98)	191 (64)	247 (30)
$[M-H]^+$	147 (100)	190 (9)	246 (16)
$[M-H-HCN]^+$	120 (15)	163 (<2)	219 (3)
$[M-H-MeCN]^+$	106 (65)	149 (<2)	205 (<2)
$[M-R]^+$	133 (38)	176 (50)	218 (21)
$[M-R-C_6H_4]^+$	57 (4)	100 (60)	142 (100)
$[M-NR_2]^+$	104 (31)	147 (100)	175 (56)
$[PhNH_2]^+$	93 (44)	93 (55)	93 (40)
$[C_6H_5]^+$	77 (64)	77 (20)	77 (27)
$[NR_2]^+$	44 (40)	44 (25)	72 (98)

to that of **1**. The general routes of fragmentation of **10** and **15** are similar, and the fragments are analogous to those observed for **1**. The following common ions are found in the mass spectra: $[M]^+$, $[M-H]^+$, $[M-R]^+$ ($R = Me$ or Et), $[M-NR_2]^+$, $[NR_2]^+$, $[C_6H_5]^+$ and other fragments formed by loss of the molecules HCN, MeCN, C_2H_4 or C_2H_2 .

The principal differences between the mass spectrum of formamidine **1** and those of guanidines **10** and **15** are ion intensities (Table 1). For formamidine **1**, intensities of the $[M]^+$ and $[M-H]^+$ ions are considerably greater than those of the $[M-R]^+$ ($R = Me$ or Et) $[M-R-Ph]^+$ and $[M-NR_2]^+$ ions. The $[M-H]^+$ ion is the base peak for **1**. For guanidines **10** and **15**, loss of the dialkylamino group is more important than loss of the H atom. The relative abundance of the $[M-H]^+$ ion is lower than 20%, whereas that of the $[M-NR_2]^+$ ion is larger than 50%. The $[M-NR_2]^+$ ion is the base peak for **10** and a major peak for **15**. The relative abundance of the $[M-R]^+$ and $[M-R-C_6H_4]^+$ ions is also larger for guanidines than for formamidine. The $[M-R-C_6H_4]^+$ ion is the base peak for **15** and a very important peak for **10**. This means that the principal route of fragmentation (loss of H atom), proposed by Grützmacher and Kuschel for N^1,N^1 -dimethyl- N^2 -phenylformamidines,^[9] is not the favored one for guanidines. This change of the favored route of fragmentation when proceeding from formamidines to guanidines may be explained in particular by the cross $n-\pi$ conjugation, which is possible for guanidines but is absent for formamidines (Scheme 1).

Molecular ions

Geometries of molecular ions $[M]^+$ of N^1,N^1 -dimethyl- N^2 -phenylformamidine (**1**) and 1,1,3,3-tetramethyl-2-phenylguanidine (**10**) were optimized *in vacuo* at the DFT(B3LYP)/6-31+G** level. Thermodynamic parameters such as the enthalpy (H), entropy term (TS) and Gibbs energy (G), and also the Mulliken atomic charges for heavy atoms (C and N), calculated at the same level of theory, are given in Fig. 1. Comparison of the DFT data shows evidently stronger variation of the charge at the ring C atoms for guanidine radical cation **10a** (from -0.926 to $+0.937$) than for formamidine radical cation **1a** (from -0.491 to $+0.574$). This variation confirms stronger electronic substituent effect of the cross $n-\pi$ conjugated guanidine group than the $n-\pi$ conjugated formamidine group. Consequently, for **1a**, the charge of the N atom linked to the Ph ring has still negative value (-0.213), whereas that for **10a** becomes already positive ($+0.040$). A change of the charge also takes place for the functional C atom from the

**Figure 1.** Mulliken atomic charges (C and N atoms) and thermodynamic parameters (H , TS and G in kcal mol^{-1}) for molecular ions of N^1,N^1 -dimethyl- N^2 -phenylformamidine (**1a**) and 1,1,3,3-tetramethyl-2-phenylguanidine (**10a**) estimated at the DFT(B3LYP)/6-31+G** level.**Table 2.** CN bond lengths (in Å) for molecular fragments $[M]^+$ of N^1,N^1 -dimethyl- N^2 -phenylformamidine (**1a**) and 1,1,3,3-tetramethyl-2-phenylguanidine (**10a**) estimated at the DFT(B3LYP)/6-31+G** level

Bond	1a ($Y = H$)	10a ($Y = NMe_2$)	Δ
C(1)-N(7)	1.351	1.338	+0.013
C(8)-N(7)	1.326	1.368	-0.042
C(8)-N(9)	1.324	1.347 ^a	-0.023
C(10)-N(9)	1.467	1.471 ^a	-0.004
C(11)-N(9)	1.467	1.471 ^a	-0.004

^a The same value is found for the $Y = NMe_2$ group.

positive value ($+0.056$) for **1a** to the negative value (-0.158) for **10a**. The charges of the N atoms in the NMe_2 groups are negative for both **1a** (-0.016) and **10a** (-0.028 and -0.056). The observed similarities and differences may influence the bond strength and the favored routes of fragmentation.

Additional information may be derived from variations of the CN bond lengths for formamidine (**1a**) and guanidine (**10a**) radical cations (Table 2). Generally, the CN bond lengths for **10a** are longer than those for **1a**. Exception is the C(1)-N(7) bond, which is shorter for cross $n-\pi$ conjugated **10a**. Longer C(8)-N(9) bond for **10a** (by 0.023 Å) may indicate lower energy of this bond and easier fragmentation of the molecular $[M]^+$ ion to the $[M-NMe_2]^+$ fragment by loss of the NMe_2 neutral radical.

Indeed, plots of the energy (Fig. 2) as function of the bond length between the C(8) and N(9) atoms of N^1,N^1 -dimethyl- N^2 -phenylformamidine (solid line) and 1,1,3,3-tetramethyl-2-phenylguanidine radical cations (dotted line) confirm the lower dissociation energy for **10a** than for **1a**. The two curves were computed *in vacuo* at the DFT(B3LYP)/6-31+G** level by performing a series of constrained energy minimization with the C(8)-N(9) distances fixed at a given value (from 1.0 to 3.0 Å)

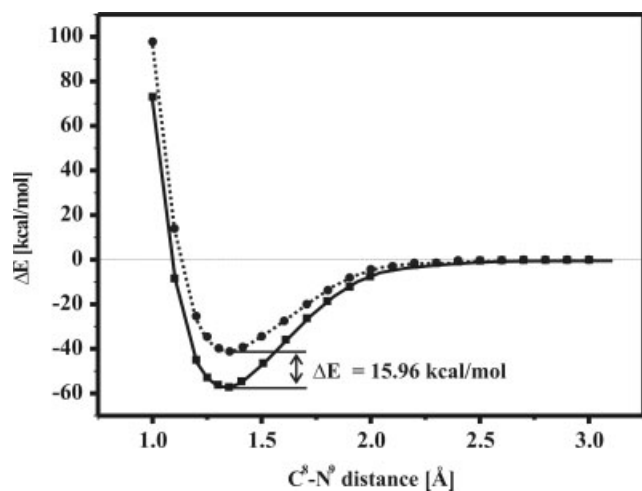


Figure 2. Plots of the energy as function of the C(8)-C(9) bond lengths for N^1,N^1 -dimethyl- N^2 -phenylformamide (solid line) and for 1,1,3,3-tetramethyl-2-phenylguanidine (dotted line). Filled squares and circles represent points where the DFT(B3LYP)/6-31+G** energies were calculated. Numbers of atoms are taken from structure given in Table 2.

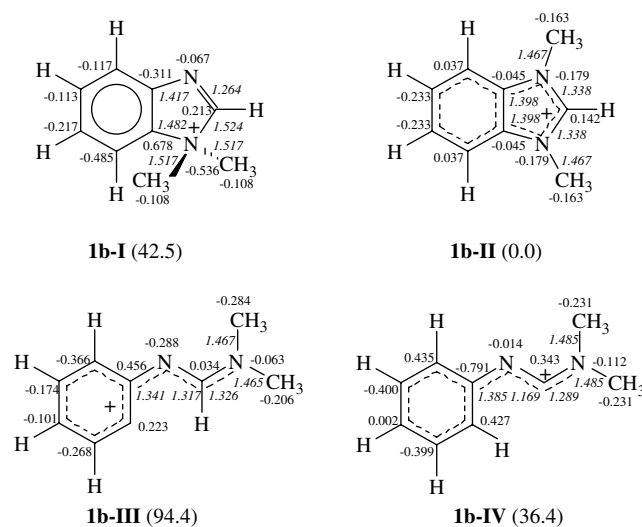
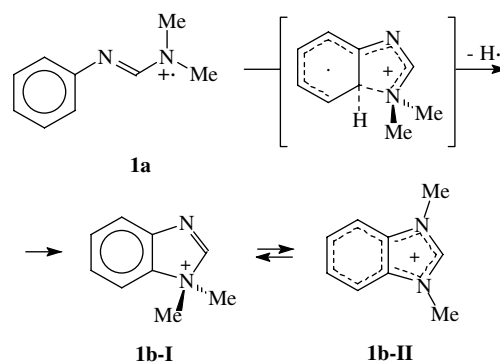


Figure 3. Four structures (I–IV) for the $[M-H]^+$ fragment of N^1,N^1 -dimethyl- N^2 -phenyl-formamide (**1b**). The CN bond lengths (in italic, Å) are placed near the corresponding bonds. The Mulliken charges are near the C and N atoms. The relative Gibbs energies (in kcal mol $^{-1}$) are given in parentheses near the number of structure. All data are calculated at the DFT(B3LYP)/6-31+G** level.

and by optimizing the remaining degrees of freedom. At larger distances, the two curves overlap each other. Very deep minima are observed in both cases at a distance about 1.35 Å. A minimum for formamide is also broader than for guanidine. The difference in the depth of these minima is about 16 kcal mol $^{-1}$, suggesting that there is a stronger bond between the C(8) and C(9) atoms for formamide (solid line) than for guanidine (dotted line). This means that more energy is needed for the NMe $_2$ detachment for formamide than for guanidine.

$[M-H]^+$ fragments

Four structures (I–IV in Fig. 3) were considered at the DFT(B3LYP)/6-31+G** level for the $[M-H]^+$ ion of N^1,N^1 -dimethyl-



Scheme 4. Formation of benzimidazolium ions.

N^2 -phenylformamide (**1b**): two bicyclic structures (I and II) in which the formamide group together with the Ph ring forms the benzimidazolium ions, and two structures with the acyclic formamide group (III and IV). In the structure I, the two Me groups are at the same N atom, similarly as in the parent molecular fragment **1b**. The benzimidazolium ion I may be formed by a formal intramolecular (cyclic) aromatic substitution reaction within the radical cation $[M]^{\bullet+}$, as it has been proposed by Grützmacher and Kuschel^[9–12] (Scheme 4). Intramolecular rearrangement of I, i.e. transfer of the Me group from one to the other N atom similar to tautomeric conversion, leads to the more symmetric benzimidazolium ion II, where the Me groups are at different N atoms.^[9] DFT calculations indicate that the II ion is thermodynamically more favorable than I by 42.5 kcal mol $^{-1}$. Variations of the Mulliken charges for the C and N atoms are smaller for II (from -0.233 to $+0.142$ and -0.179 , respectively) than for I (from -0.485 to $+0.678$ and from -0.536 to -0.067 , respectively). Similarly, the CN bond lengths vary in smaller degree for II (from 1.338 to 1.467 Å) than for I (from 1.264 to 1.517 Å). High symmetry stabilizes well the benzimidazolium ion II.

The structures III and IV may be formed by direct loss of the H atom, one linked to the ring *ortho*-C atom (III), and the other to the C functional atom (IV). Both structures, however, display greater variations of the Mulliken charges for C (from -0.366 to $+0.456$ and from -0.791 to $+0.435$, respectively) and N (from -0.288 to -0.063 and from -0.112 to -0.014 , respectively) atoms and greater variations of the CN bond lengths (from 1.317 to 1.467 Å and from 1.169 to 1.485 Å, respectively) than the benzimidazolium ion II. They have also larger Gibbs energies than II by 94.4 and 36.4 kcal mol $^{-1}$, respectively. Hence, one may conclude that for parent formamide **1**, the $[M-H]^+$ ion prefers the benzimidazolium structure II in the gas phase. Similar trend is found for substituted formamides (**2–9**) at the AM1 level. The stability order of the $[M-H]^+$ structures is as follows: II > IV > I > III. The structures I have larger energies than II by 30–32 kcal mol $^{-1}$ (30.8 kcal mol $^{-1}$ for **1**). Energies of III and IV are larger than II by 78–89 and 15–18 kcal mol $^{-1}$ (86.1 and 18.4 kcal mol $^{-1}$ for **1**), respectively. Although the AM1 method gives lower relative energies than the DFT method, it reproduces well the stabilities order and indicates the same favored structure II for the $[M-H]^+$ ion for all derivatives in series of formamides studied here.

In the case of 1,1,3,3-tetramethyl-2-phenylguanidine (**10**), three structures are possible for the $[M-H]^+$ ion similar to structures I–III for formamides: two bicyclic benzimidazolium structures (I and II) and one monocyclic structure with the acyclic guanidine group (III). The benzimidazolium ions I and II may be formed by similar formal intramolecular substitution reaction within the

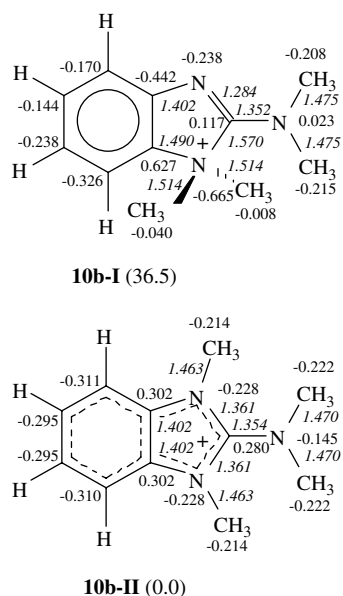


Figure 4. Two benzimidazolium ions $[M-H]^+$ for 1,1,3,3-tetramethyl-2-phenylguanidine (**10b-I** and **10b-II**). The CN bond lengths (in italic, Å) are placed near the corresponding bonds. The Mulliken charges are near the C and N atoms. The relative Gibbs energies (in kcal mol⁻¹) are given in parentheses near the number of structure. All data are calculated at the DFT(B3LYP)/6-31+G** level.

Table 3. Enthalpies (*H*), entropy terms (*TS*) and Gibbs energies (*G*) for benzimidazolium structures $[M-H]^+$ of *N*¹,*N*¹-dimethyl-*N*²-phenylformamide (**1b-I** and **1b-II**) and 1,1,3,3-tetramethyl-2-phenylguanidine (**10b-I** and **10b-II**) calculated at the DFT(B3LYP)/6-31+G** level (in kcal mol⁻¹)

Structure	<i>H</i>	<i>TS</i>	<i>G</i>	ΔH^a	$T\Delta S^a$	ΔG^a
1b-I	-287803.2	27.3	-287830.6	41.8	-0.9	42.5
1b-II	-287845.0	28.2	-287873.1	0.0	0.0	0.0
10b-I	-371838.7	33.6	-371872.2	35.5	-0.8	36.5
10b-II	-371874.2	34.4	-371908.7	0.0	0.0	0.0

^a Relative value between structure **I** and **II**.

molecular ion $[M]^+\bullet$ and by similar intramolecular rearrangement as it has been proposed for formamidines (Scheme 4). As it could be expected, the monocyclic structure **III** has considerably larger energy than the benzimidazolium ions (by more than 60 kcal mol⁻¹ at the AM1 level). Thus, it was not considered at the DFT level. Geometries were optimized solely for benzimidazolium ions (**I** and **II**). The DFT results are given in Fig. 4 and Table 3. Due to high symmetry, the benzimidazolium ion **II** has smaller variations of the Mulliken charges for the C (from -0.311 to +0.302) and N atoms (from -0.228 to -0.145) and smaller variations of the CN bond lengths (from 1.361 to 1.470 Å) than **I** (from -0.442 to +0.627, from -0.665 to +0.023 and from 1.284 to 1.570 Å, respectively). The structure **II** has also lower Gibbs energy than **I** by 36.5 kcal mol⁻¹. Similar trend is found for guanidine **15** as well as for substituted guanidines **11–14**. The stability order of the $[M-H]^+$ structures for guanidines **10–15** is as follows: **II** > **I** > **III**. The structures **I** have larger energies than **II** by 27–31 kcal mol⁻¹ (27.8 kcal mol⁻¹ for **10** and 30.7 kcal mol⁻¹ for **15**). Energies of **III** are larger than **II** by 85–96 kcal mol⁻¹ (93.2 for

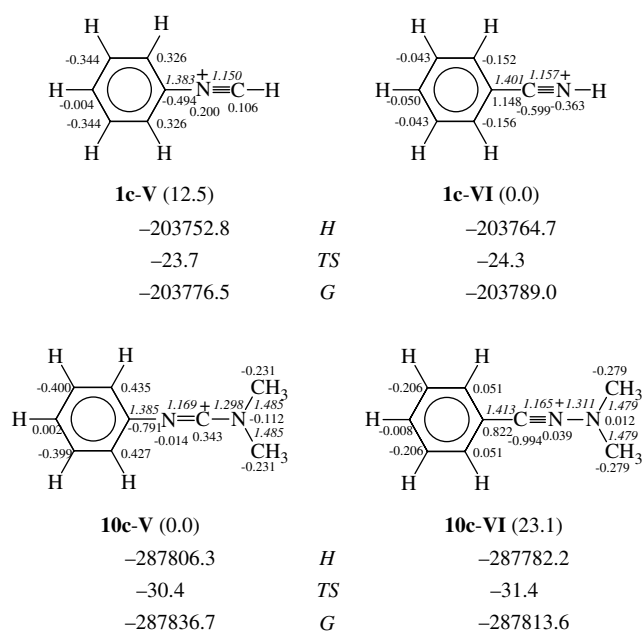


Figure 5. Two structures (benzisonitrilium **V** and benzonitrilium **VI**) for the $[M-NMe_2]^+$ fragment of *N*¹,*N*¹-dimethyl-*N*²-phenylformamide (**1c**) and 1,1,3,3-tetramethyl-2-phenylguanidine (**10c**). The CN bond lengths (in italic, Å) are placed near the corresponding bonds. The Mulliken charges are near the C and N atoms. The relative Gibbs energies (in kcal mol⁻¹) are given in parentheses near the number of structure. Thermodynamic parameters (*H*, *TS* and *G* in kcal mol⁻¹) are below the structures. All data are calculated at the DFT(B3LYP)/6-31+G** level.

10 and 95.8 kcal mol⁻¹ for **15**). The DFT and AM1 results indicate that the $[M-H]^+$ ion prefers the benzimidazolium structure **II** for all guanidines studied here.

$[M-NMe_2]^+$ fragments

Loss of the NMe_2 neutral radical from the molecular ion $[M]^+\bullet$ of parent formamide **1** leads to the benzonitrilium ion **1c-V**, which may rearrange to the benzonitrilium ion **1c-VI**. Both ions are stable at the DFT level. The variations of the Mulliken charges, the CN bond lengths and thermodynamic parameters are given in Fig. 5. The benzonitrilium ion possesses a lower Gibbs energy (by 12.6 kcal mol⁻¹). Similar results are found for substituted formamidines (**2–9**) at the AM1 level. For all derivatives, the benzonitrilium ion **VI** has lower energy than the benzisonitrilium ion **V** by 13–16 kcal mol⁻¹. Interestingly, the AM1 method reproduces quite well the relative energy for **1** (13.6 kcal mol⁻¹). It is larger than the DFT value by solely 1 kcal mol⁻¹. Hence, one can conclude that the $[M-NMe_2]^+$ ion prefers the benzonitrilium ion **VI** for all formamidines in studied series.

In the case of parent guanidine **10** (Fig. 5), we considered at the DFT level the same benzisonitrilium structure **10c-V** for the $[M-NMe_2]^+$ fragment ($m/z = 147$) as **1b-IV** for the $[M-H]^+$ fragment ($m/z = 147$) of parent formamide which may be formed from the molecular ion $[M]^+\bullet$ by loss of the H atom at the functional C atom. The benzisonitrilium ion **10c-VI** has a lower energy than the corresponding benzonitrilium ion by 23.1 kcal mol⁻¹ at the DFT level. The same trend is found for substituted guanidines (**11–14**). Energies of the benzisonitrilium ions are lower than those of benzonitrilium ions by 21–22 kcal mol⁻¹ at the AM1 level (22.0 kcal mol⁻¹ for **10**).

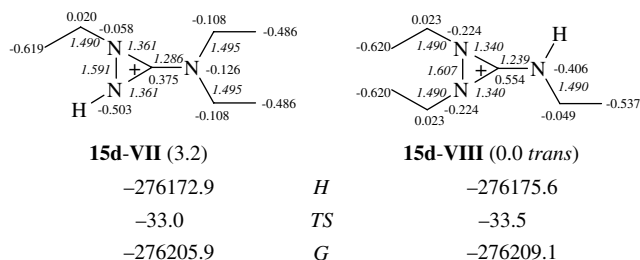


Figure 6. Two cyclic structures (**15d-VII** and **15d-VIII**) for the $[C_7H_{16}N_3]^+$ fragment of TEPG. The CN bond lengths (in italic, Å) are placed near the corresponding bonds. The Mulliken charges are near the C and N atoms. The relative Gibbs energies (in kcal mol⁻¹) are given in parentheses near the number of structure. Thermodynamic parameters (*H*, *TS* and *G* in kcal mol⁻¹) are below the structures. All data are calculated at the DFT(B3LYP)/6-31+G** level.

These results indicate a change of the favored structure for the $[M-NMe_2]^+$ fragment when going from DMAFs (benzonitrilium ion) to TMAGs (benzisonitrilium ion).

$[M-Et-C_6H_4]^+$ fragment

The $[C_7H_{16}N_3]^+$ fragment ($m/z = 142$) is the base peak for TEPG (**15**). At the AM1 level, the cyclic structures have lower energy than the acyclic ones by more than 20 kcal mol⁻¹. In fact, the latter structures are unstable at the DFT level and during geometry optimization shift to the corresponding cyclic structures (**VII** and **VIII** in Fig. 6). The cyclic structures differ by position of the ethyl groups, which may be interconverted by group switching similar to tautomerism. The different positions of the Et groups affect the Mulliken charges as well as the CN and NN bond lengths. They influence also the stabilities of ions. At the DFT level, the structure **VIII** with the Et groups at the ring N atoms in *trans* position has lower Gibbs energy than **VII** by 3.2 kcal mol⁻¹. The *cis* isomer of **VIII** has larger Gibbs energy than the *trans* one by 9.4 kcal mol⁻¹. Our DFT results indicate that the $[C_7H_{16}N_3]^+$ fragment prefers the structure **VIII** with the Et groups at the ring N atoms in *trans* position.

Substituent effect on ion abundances in DMAF

Mass spectrometric fragmentation of DMAFs has been discussed by Grützmaier and Kuschel more than 30 years ago,^[9–12] and also reviewed by Haefelinger^[30] in 1975 and by Fornarini in 1991.^[31] However, substituent effects on ion abundances in mass spectra have been discussed solely qualitatively to prove the proposed mechanism of the favored routes of fragmentation and the formation of benzimidazolium ions $[M-H]^+$ by a formal intramolecular (cyclic) aromatic substitution reaction within the radical cation $[M]^+•$ (Scheme 4). Grützmaier and Kuschel^[9–12] observed that the intensity of the cyclic ions $[M-H]^+$ is strongly reduced by electron-donating substituents such as 4-OH, 4-OMe, 4-NMe₂ and 4-N=CHNMe₂. Other substituents induce small change in intensity, e.g. 4-Me and 4-Cl slightly reduce the $[M-H]^+$ intensity, and 3-COOMe, 3-COMe and 3-Cl slightly increase the $[M-H]^+$ intensity.

During our investigations of mass spectra of DMAFs (Table 4), *para*-substituted at the phenyl ring (**1–9**), we observed interesting linear relationships between $\log\{[M-H]^+/[M]^+•\}$ and substituent constants (Fig. 7). For σ_p^+ constants,^[32] the relation is significant: $\log\{[M-H]^+/[M]^+•\} = -0.25 + 0.34 \cdot \sigma_p^+$ with $r = 0.919$ ($n = 9$).

Table 4. Substituent constants (σ_p^+ and σ_R^+)^[32] and selected spectral data for DMAFs

(a) Favored fragments					
Z	σ_p^+	σ_R^+	$[M]^+•$	$[M-H]^+$	$\log\{[M-H]^+/[M]^+•\}$
4-NO ₂	0.79	0.00	193 (100)	192 (87)	-0.06
4-CN	0.66	0.00	173 (81)	172 (68)	-0.08
4-CF ₃	0.61	0.00	216 (100)	215 (88)	-0.06
4-Cl	0.11	-0.17	182 (100)	181 (55)	-0.26
4-F	-0.07	-0.25	166 (100)	165 (50)	-0.30
H	0.00	0.00	148 (97)	147 (100)	0.01
4-Me	-0.31	-0.08	162 (100)	161 (60)	-0.22
4-OMe	-0.78	-0.42	178 (36)	177 (9)	-0.60
4-NMe ₂	-1.70	-0.64	191 (100)	190 (13)	-0.89
(b) Other important fragments					
Z	$[M-Me]^+$	$[M-NMe_2]^+$	$\log\{[M-Me]^+/[M]^+•\}$	$\log\{[M-NMe_2]^+/[M]^+•\}$	
4-NO ₂	178 (53)	149 (6)	-0.28	-1.22	
4-CN	158 (45)	129 (20)	-0.26	-0.61	
4-CF ₃	201 (34)	172 (8)	-0.47	-1.10	
4-Cl	167 (70)	138 (31)	-0.15	-0.51	
4-F	151 (66)	122 (41)	-0.18	-0.39	
H	133 (37)	104 (39)	0.42	-0.40	
4-Me	147 (43)	118 (21)	-0.37	-0.68	
4-OMe	163 (39)	134 (8)	0.03	-0.65	
4-NMe ₂	176 (74)	147 (14)	-0.13	-0.85	

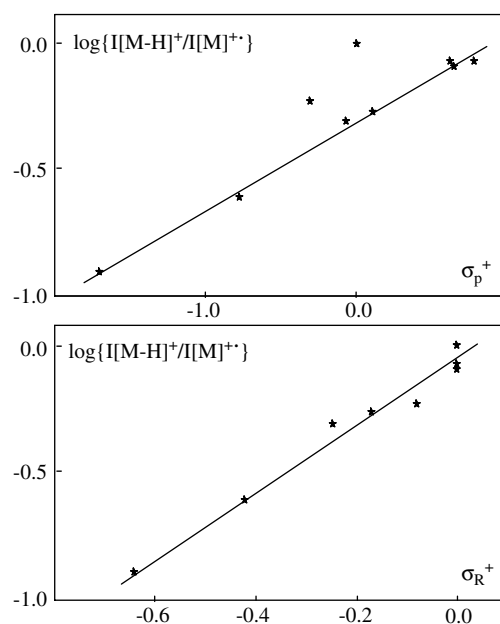


Figure 7. Relations between $\log\{[M-H]^+/[M]^+•\}$ of DMAFs and substituent constants.^[32]

Although for all substituted derivatives the benzimidazolium ion **II** seems to be favored at the quantum-chemical levels, for unknown reason, two points (for compounds **1** and **4**) slightly deviate from this relation. When these points are neglected, the linearity is better: $\log\{[M-H]^+/[M]^+•\} = -0.30 + 0.35 \cdot \sigma_p^+$ with $r = 0.997$ ($n = 7$). In order to identify the specific substituent

Table 5. Selected mass spectrometric data for TMAGs^a

Ion	10	11	12	13	14 ^b	
[M] ⁺	191 (64)	221 (100)	205 (84)	209 (62)	225 (54)	227 (22)
[M-H] ⁺	190 (9)	220 (20)	204 (16)	208 (14)	224 (11)	226 (25) ^c
[M-Me] ⁺	176 (50)	206 (87)	190 (64)	194 (53)	210 (49)	212 (17)
[M-NMe ₂] ⁺	147 (100)	177 (75)	161 (100)	165 (100)	181 (100)	183 (33)
[M-NMe ₂ -Me] ⁺	132 (77)	162 (87)	146 (83)	150 (94)	166 (96)	168 (27)
[M-NMe ₂ -HCN] ⁺	120 (65)	150 (99)	134 (88)	138 (59)	154 (67)	156 (23)
[M-NMe ₂ -MeCN] ⁺	106 (21)	136 (41)	120 (30)	124 (20)	140 (23)	142 (7)
[M-NMe ₂ -Z] ⁺	–	147 (68)	146 (83)	146 (<2)	146 (8)	148 (<2)
[ZC ₆ H ₄ NH ₂] ⁺	93 (55)	123 (3)	107 (8)	111 (4)	127 (4) ^d	129 (<2)
[ZC ₆ H ₄ NH] ⁺	92 (16)	122 (19)	106 (21)	110 (16)	126 (12)	128 (4)
[ZC ₆ H ₄ N] ⁺	91 (12)	121 (14)	105 (10)	109 (14)	125 (13)	127 (4) ^d
[ZC ₆ H ₄] ⁺	77 (20)	107 (<2)	91 (38)	95 (11)	111 (11)	113 (<2)
[ZC ₅ H ₅] ⁺	66 (18)	96 (<2)	80 (2)	94 (<2)	100 (60) ^e	102 (4)
[ZC ₅ H ₄] ⁺	65 (9)	95 (2)	79 (5)	83 (7)	99 (6)	101 (5)
[C ₅ H ₁₂ N ₂] ⁺ /[C ₄ H ₁₀ N ₃] ⁺	100 (60)	100 (59)	100 (61)	100 (42)		100 (60) ^e
[C ₆ H ₅] ⁺	77 (20)	77 (3)	77 (8)	77 (<2)		77 (<2)
[C ₅ H ₅] ⁺	65 (9)	65 (5)	65 (11)	65 (<2)		65 (<2)
[C ₄ H ₃] ⁺	51 (8)	51 (3)	51 (2)	51 (<2)		51 (<2)
[C ₂ H ₆ N] ⁺	44 (25)	44 (24)	44 (22)	44 (20)		44 (26)
[C ₂ H ₄ N] ⁺	42 (24)	42 (21)	42 (18)	42 (16)		42 (19)

^a Only significant ions ($m/z > 40$) are listed.

^b Peaks corresponding to ³⁵Cl and ³⁷Cl are listed.

^c The intensity is the sum of intensities of two peaks: [M-H]⁺ with ³⁷Cl and [M+H]⁺ with ³⁵Cl.

^d The intensity is the sum of intensities of two isotopic peaks: [³⁵ClC₆H₄NH₂]⁺ and [³⁷ClC₆H₄N]⁺.

^e The intensity is the sum of intensities of two peaks: [³⁵ClC₅H₅]⁺ and [C₅H₁₂N₂]⁺/[C₄H₁₀N₃]⁺.

effects that influence ion abundances in DMAFs, we considered also relations with σ_α , σ_F and σ_R^+ , which correspond respectively to the polarizability, field/inductive and resonance substituent effects.^[32] A linear relation was found with σ_R^+ constants: $\log\{[M-H]^+/[M]^+\} = -0.05 + 1.29 \cdot \sigma_R^+$ with $r = 0.989$ ($n = 9$). For substituents Z = 4-NO₂, 4-CN, 4-CF₃ and H, the substituent constants σ_R^+ are close to zero, and also, the $\log\{[M-H]^+/[M]^+\}$ values are close to zero, although the ion intensity of the favored fragments are not the same. A plot of $\log\{[M-H]^+/[M]^+\}$ vs σ_α and σ_F shows a large scatter, and adding these parameters to the simple mono-parametric equation with σ_R^+ does not improve the precision. Although our mass spectra of DMAFs were recorded under different conditions (FT-ICR) than those reported by Grützmaier and Kuschel (sector instrument, Varian MAT),^[9] there is a linear relation between our and earlier data: $\log\{[M-H]^+/[M]^+\}$ (this work) = $-0.39 + 1.16 \log\{[M-H]^+/[M]^+\}$ (G&K) with $r = 0.984$ ($n = 6$).

It is interesting to mention here that the DMAFs series does not follow general behavior observed earlier in the literature^[6] and shows that the substituent is not significantly involved in secondary dissociation(s). The linear relation of the $\log\{[M-H]^+/[M]^+\}$ values with σ_p^+ constants, and more precisely with σ_R^+ constants, confirms quantitatively the effect of electron-donating substituents and substantiates the mechanism proposed by Grützmaier and Kuschel.^[9–12] The formation of the cyclic benzimidazolium ions [M-H]⁺ during mass spectral fragmentation of DMAFs is more favored by electron-accepting than by electron-donating substituents (see ion intensities in Table 4). On the other hand, lack of linear relations between the $\log\{[M-Me]^+/[M]^+\}$ values and the σ_p^+ and σ_R^+ constants, and also between the $\log\{[M-Me]^+/[M]^+\}$ values and the σ_α and σ_F constants,

suggests that the [M-Me]⁺ fragments have not benzimidazolium structure like the [M-H]⁺ ions and/or that the mechanism of formation of the [M-Me]⁺ fragments is different than that of the [M-H]⁺ ions. For less important [M-NMe₂]⁺ fragments, relations of the $\log\{[M-NMe_2]^+/[M]^+\}$ values and the substituent constants (σ_p^+ , σ_α , σ_F and σ_R^+) are also not linear.

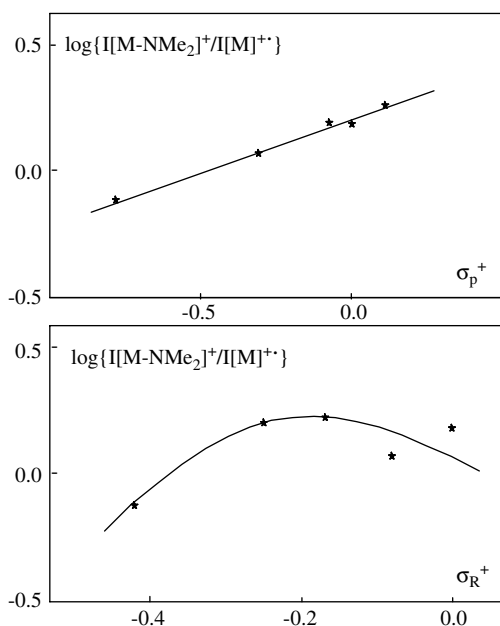
Substituent effect on ion abundances in TMAG

In the TMAGs series (11–14), fragmentation is similar to that of the parent compound 10 (Table 5). Except for 11, the [M-NMe₂]⁺ ion is the base peak. The electron-donating OMe group for 11 favors the molecular [M]⁺ ion which is the base peak, and the relative abundance of the [M-NMe₂]⁺ ion is reduced to 75%. For the other substituents Me, F, Cl and H, the molecular ion abundance varies from 54 to 84%. The [M-H]⁺ ion is present in the mass spectrum of all TMAGs, but its relative abundance is not larger than 20%. Loss of the NMe₂ group is the principal fragmentation. The fragmentation of the [M-NMe₂]⁺ ion is followed by the loss of the Me group, and of the HCN and MeCN molecules. The fragments [M-NMe₂]⁺, [M-NMe₂-Me]⁺, [M-NMe₂-HCN]⁺ and [M-NMe₂-MeCN]⁺ can be considered as typical for mass spectra of TMAGs. Major fragments are also [M-Me]⁺ and [C₅H₁₂N₂]⁺/[C₄H₁₀N₃]⁺ ($m/z = 100$). Their relative abundances are very significant (between 20 and 99%). The typical fragment [C₂H₆N]⁺ ($m/z = 44$) is present in the mass spectrum of each TMAG and its abundance is between 20 and 30%.

For TMAGs, the fragmentation with loss of the H atom is not as important as for DMAFs. Hence, substituent Z at the phenyl ring has no significant effect on the $\log\{[M-H]^+/[M]^+\}$ values which vary solely from -0.64 for F to -0.85 for H

Table 6. Substituent constants (σ_p^+ and σ_R^+)^[32] and selected spectral data for TMAGs

Z	σ_p^+	σ_R^+	$\log\{I[M-H]^+ / I[M]^{+\bullet}\}$	$\log\{I[M-Me]^+ / I[M]^{+\bullet}\}$	$\log\{I[M-NMe_2]^+ / I[M]^{+\bullet}\}$
4-Cl	0.11	-0.17	-0.69	-0.04	0.27
4-F	-0.07	-0.25	-0.64	-0.07	0.21
H	0.00	0.00	-0.85	-0.11	0.19
4-Me	-0.31	-0.08	-0.72	-0.12	0.08
4-OMe	-0.78	-0.42	-0.70	-0.06	-0.12

**Figure 8.** Relations between $\log\{I[M-NMe_2]^+ / I[M]^{+\bullet}\}$ of TMAGs and substituent constants.^[32]

(Table 6). Linear relationships with σ_p^+ ($r = 0.161$) and σ_R^+ ($r = 0.659$) constants are not significant for TMAGs. Similarly, substituent Z at the phenyl ring has no significant effect on the $\log\{I[M-Me]^+ / I[M]^{+\bullet}\}$ values which vary solely from -0.04 for Cl to -0.12 for Me. Quite a different situation takes place for the favored route of fragmentation, i.e. loss of the NMe_2 group. The $\log\{I[M-NMe_2]^+ / I[M]^{+\bullet}\}$ values correlate well with σ_p^+ constants (Fig. 8): $\log\{I[M-NMe_2]^+ / I[M]^{+\bullet}\} = 0.22 + 0.43 \cdot \sigma_p^+$ with $r = 0.993$ ($n = 5$). Relation with σ_R^+ is not linear. This suggests that substituent Z at the Ph ring may affect the loss of the NMe_2 radical at the C functional atom (separated by the N atom from the Ph ring) not only by resonance but also by field/inductive effect. Unfortunately, five points are not sufficient to perform valuable multiparameter analysis of substituent effects, in order to separate the resonance and field/inductive contributions.

Conclusions

Investigations of electron-ionization mass spectra for analogous series of DMAFs and TMAGs showed an interesting change of the preferential routes of fragmentation from favored formation of the $[M-H]^+$ benzimidazolium ions for DMAFs to favored formation of the $[M-NMe_2]^+$ benzisonitrilium ions for TMAGs.

This change may be explained by cross $n-\pi$ conjugation present in guanidines and absent in formamidines (Scheme 1). The cross $n-\pi$ conjugation affects the Mulliken atomic charges, the CN bond lengths, and consequently, the bond strength and fragmentation. Linear relationships between the logarithm of ion abundances ratio and substituent constants are observed for the favored fragments. For TEPG, the preferential routes of fragmentation are slightly different than those for TMAGs. Larger alkyl groups at the N atom increase electronic effects and change the stability fragments. Although the $[M-NEt_2]^+$ ion is still important, the $[C_7H_{16}N_3]^+$ fragment is favored.

Acknowledgements

DFT calculations were conducted using the resources of 45-processor Beowulf cluster at the Faculty of Chemistry (University of Gdańsk) and the Informatics Center of the Metropolitan Academic Network (IC MAN, Gdańsk).

References

- [1] G. Haeflinger, F. K. H. Kuske, in *The Chemistry of Amidines and Imidates*, Vol. 2, Chap. 1 S. Patai, Z. Rappoport (Eds). Wiley: Chichester, **1991**.
- [2] E. D. Raczyńska, J.-F. Gal, P.-C. Maria, M. Szeląg. *Croat. Chem. Acta* **2009**, *82*, 87.
- [3] E. D. Raczyńska, M. Decouzon, J.-F. Gal, P.-C. Maria, G. Gelbard, F. Vielfaure-Joly. *J. Phys. Org. Chem.* **2001**, *14*, 25.
- [4] I. Kaklurand, I. A. Koppel, A. Kütt, E.-I. Rööm, T. Rodima, I. Koppel, M. Mishima, I. Leito. *J. Phys. Chem. A* **2007**, *111*, 1245.
- [5] Z. Glasovac, V. Štrukil, M. Eckert-Maksić, D. Schröder, M. Kaczorowska, H. Schwarz. *Int. J. Mass Spectrom.* **2008**, *270*, 39.
- [6] M. M. Bursey, in *Advances in Linear Free Energy Relationships*, Chap. 10, N. B. Chapman, J. Shorter (Eds). Plenum Press: London and New York, **1972**.
- [7] A. G. Harrison. *J. Mass Spectrom.* **1999**, *34*, 577.
- [8] A. K. Bose, I. Kugajevsky, P. T. Funke, K. G. Das. *Tetrahedron Lett.* **1965**, *35*, 3065.
- [9] H. F. Grützmacher, H. Kuschel. *Org. Mass Spectrom.* **1970**, *3*, 605.
- [10] H. Kuschel, H. F. Grützmacher. *Org. Mass Spectrom.* **1974**, *9*, 395.
- [11] H. Kuschel, H. F. Grützmacher. *Org. Mass Spectrom.* **1974**, *9*, 403.
- [12] H. Kuschel, H. F. Grützmacher. *Org. Mass Spectrom.* **1974**, *9*, 408.
- [13] M. Medved, S. Stavber, V. Kramer, L. Benčić, J. Marsel. *Croat. Chem. Acta* **1977**, *49*, 415.
- [14] E. D. Raczyńska, M. Decouzon, J.-F. Gal, P.-C. Maria, R. W. Taft. *J. Mass Spectrom.* **1998**, *33*, 1029.
- [15] J. Oszczapowicz, E. Raczyńska. *Pol. J. Chem.* **1983**, *57*, 419.
- [16] H. Borgarello, R. Houriet, E. D. Raczyńska, T. Drapała. *J. Org. Chem.* **1990**, *55*, 38.
- [17] R. W. Taft, E. D. Raczyńska, P.-C. Maria, I. Leito, J.-F. Gal, M. Decouzon, T. Drapała, F. Anvia. *Pol. J. Chem.* **1995**, *69*, 41.
- [18] H. Bredereck, K. Bredereck. *Chem. Ber.* **1961**, *94*, 2278.
- [19] J. Oszczapowicz, J. Osek. *Pol. J. Chem.* **1983**, *57*, 93.
- [20] E. D. Raczyńska, P.-C. Maria, J.-F. Gal, M. Decouzon. *J. Phys. Org. Chem.* **1994**, *7*, 725.
- [21] M. Decouzon, J.-F. Gal, S. Geribaldi, P.-C. Maria, M. Rouillard. *Spectra* **2000** **1989**, *17*, 51.
- [22] M. Decouzon, J.-F. Gal, P.-C. Maria, E. D. Raczyńska. *Org. Mass Spectrom.* **1991**, *26*, 1127.
- [23] M. J. S. Dewar, E. G. Zoebisch, E. F. Healy, J. J. P. Stewart. *J. Am. Chem. Soc.* **1985**, *107*, 3902.
- [24] Autodesk, Inc. *HyperChem*. Autodesk, Inc.: Sausalito, CA, **1992**.
- [25] R. G. Parr, W. Yang. *Density Functional Theory of Atoms and Molecules*. Oxford University Press: New York, **1989**.
- [26] A. D. Becke. *J. Chem. Phys.* **1993**, *98*, 5648.
- [27] C. Lee, W. Yang, R. G. Parr. *Phys. Rev. B* **1988**, *37*, 785.
- [28] W. J. Hehre, L. Radom, P. v. R. Schleyer, J. A. Pople. *Ab initio Molecular Theory*. Wiley: New York, **1986**.

- [29] M. J. Firsch, G. W. Trucks, H. B. Schlegel, G. E. Scuseria, M. A. Robb, J. R. Cheeseman, V. G. Zakrzewski, J. A. Montgomery Jr, R. E. Stratmann, J. C. Burant, S. Dapprich, J. M. Millam, A. D. Daniels, K. N. Kudin, M. C. Strain, O. Farkas, J. Tomasi, V. Barone, M. Cossi, R. Cammi, B. Mennucci, C. Pomelli, C. Adamo, S. Clifford, J. Ochterski, G. A. Petersson, P. Y. Ayala, Q. Cui, K. Morokuma, D. K. Malick, A. D. Rabuck, K. Raghavachari, J. B. Foresman, J. Cioslowski, J. V. Ortiz, A. G. Baboul, G. Liu, A. Liashenko, P. Piskorz, I. Komaromi, R. Gomperts, R. L. Martin, D. J. Fox, T. Keith, M. A. Al-Laham, C. Y. Peng, A. Nanayakkara, M. Challacombe, P. M. W. Gill, B. G. Johnson, W. Chen, M. W. Wong, J. L. Andres, C. Gonzalez, M. Head-Gordon, E. S. Replogle, J. A. Pople. Gaussian 98. Gaussian, Inc.: Pittsburgh, PA, **1998**.
- [30] G. Haefelinger, in *The Chemistry of Amidines and Imidates*, Vol. 1, Chap. 1, S. Patai (Ed). Wiley: New York, **1975**.
- [31] S. Fornarini, in *The Chemistry of Amidines and Imidates*, Vol. 2, Chap. 5, S. Patai, Z. Rappoport (Eds). Wiley: Chichester, **1991**.
- [32] C. Hansch, A. Leo, R. W. Taft. *Chem. Rev.* **1991**, *91*, 165.